



ORIGINAL ARTICLE

Structural elucidation of two intricate polycyclic polyprenylated acylphloroglucinols using quantum chemical calculations and their hypoglycemic activities



Qingqing Li^{a,1}, Shuang Yang^{a,1}, Haida Teng^b, Xueni Li^a, Wenli Xie^a, Zhili Wu^c, Guangzhong Yang^a, Jing Xu^{a,*}, Yu Chen^{b,*}

^a School of Pharmaceutical Sciences, South-Central University for Nationalities, Wuhan 430074, PR China

^b College of Chemistry and Material Sciences, South-Central University for Nationalities, Wuhan 430074, PR China

^c School of Pharmacy, Second Military Medical University, Shanghai 200433, PR China

Received 11 February 2022; accepted 15 July 2022

Available online 20 July 2022

KEYWORDS

Polycyclic polyprenylated acylphloroglucinols;
Garcinia bracteata;
Garcinia multiflora;
GIAO NMR calculations;
Hypoglycemic activity

Abstract Compounds **1-2**, the rare examples of polycyclic polyprenylated acylphloroglucinols (PPAPs) with unique 6/5/7 and 6/6 ring systems possessing unprecedented 2, 3, 12-trioxatricyclo-[5.3.1.1^{5,11}] dodecane and bicyclo-[4.4.0] decane, respectively, were isolated from the fruits of *Garcinia bracteata* and *Garcinia multiflora*, respectively. Their structures and absolute configurations were elucidated by the combination of gauge-independent atomic orbital (GIAO) NMR calculations and electronic circular dichroism (ECD) calculations. Furthermore, the hypoglycemic activity of **1** was assayed by the insulin resistance (IR)-HepG2 cell model. The results showed that compound **1** at the concentrations of 2, 4, and 6 μM could significantly promote glucose uptake dose-dependently and improve glucose metabolism disorder. Taken together, these findings suggested **1** could be a promising candidate for the treatment of diabetes mellitus.

© 2022 The Author(s). Published by Elsevier B.V. on behalf of King Saud University. This is an open access article under the CC BY-NC-ND license (<http://creativecommons.org/licenses/by-nc-nd/4.0/>).

1. Introduction

Structure determination of natural products is an essential step in the drug research and development process (Cao et al., 2021). Nuclear magnetic resonance (NMR) spectroscopy is an indispensable analytical tool to determine the structure of natural products. However, it is important to note that, although the structure determination benefits from a large number of spectral techniques available now, there are still inherent challenges in identifying their structures of the novel and complex natural products (Burns and Reynolds, 2021). Recently, a large number of structural misassignments of natural products and

* Corresponding authors.

E-mail addresses: xuj@mail.scuec.edu.cn (J. Xu), chenyuwh888@126.com (Y. Chen).

¹ These authors contributed equally to this work.

Peer review under responsibility of King Saud University.



their revisions have been reported in the literature regardless of the use of 2D-NMR techniques that are now available for structure elucidation (McAlpine et al., 2019; Chhetri et al., 2018). Therefore, it is necessary to develop better, more reliable, and more robust methods for structural identification. The density functional theory (DFT) gauge-independent atomic orbital (GIAO) NMR calculations with higher accuracy, play important roles in structural assignment for natural products. To avoid structural misassignments, the powerful approach of the combination of GIAO NMR calculations and DP4+ analysis has been developed to assist structural elucidation and revision, which possesses higher accuracy and confidence (Grimblat et al., 2015). This method has been successfully resolved many tough tasks of structural identifications of natural products, which are difficult to be solved by conventional structural elucidation methods (Marcarino et al., 2022).

Polycyclic polyprenylated phloroglucinols (PPAPs) with highly oxidized phloroglucinol-derived nuclei decorated with prenyl or geranyl side chains are a special group of hybrid natural products. Up to now, more than 800 PPAPs have been mainly isolated from the *Guttiferæ* plants with structural diversities. Most of the isolated PPAPs belong to bicyclic polyprenylated acylphloroglucinols (BPAPs) with bicyclo[3.3.1]nonane-2,4,9-trione core. In addition to the conventional [3.3.1]-type BBAPs, there are some unusual types, such as [5.3.1]-type-BPAPs, [4.3.1]-type-BPAPs, [3.2.1]-type-BPAPs, *seco*-BPAPs (Fig. S1, Supplementary Information abbreviated SI; Ciochina and Grossman, 2006; Yang et al., 2018). Owing to their attractive chemical structure and promising biological activity, BPAPs such as garcinol and isogarcinol have attracted noticeable attention from synthetic and biological communities (Phang et al., 2020; Socolsky and Plietker, 2015).

In our efforts toward new bioactive BPAPs from the *Garcinia* species, two rare BPAPs with unique 6/5/7 and 6/6 ring systems possessing unprecedented 2, 3, 12-trioxatricyclo-[5.3.1.1^{5,11}] dodecane and bicyclo-[4.4.0] decane, respectively, were obtained from the fruits of *Garcinia bracteata* and *Garcinia multiflora* respectively. Compound **1** represents the first instance of 2, 3-dioxo [5.3.1]-type-BPAPs while **2** is the first example of [4.4.0]-type-BPAPs. Their structures and absolute configurations were elucidated by the combination of gauge-independent atomic orbital (GIAO) NMR calculations and electronic circular dichroism (ECD) calculations. Moreover, the hypoglycemic activity of **1** was assayed by the insulin resistance (IR)-HepG2 cell model. This paper presented the isolation, structure elucidation, biosynthesis discussion, and biological activity of compound **1** (Fig. 1).

2. Materials and methods

2.1. General experimental procedures

Optical rotations were determined in MeOH on an Autopol IV polarimeter (Rudolph Research Analytical, Hackettstown, NJ, USA). UV spectra were obtained on a UH5300 UV-VIS Double Beam spectrophotometer (Hitachi Co., Tokyo, Japan). ECD spectra were recorded on a Chirascan Plus spectrometer (Applied Photophysics Ltd, London, England). 1D and 2D NMR spectra were recorded on a Bruker AVANCE IITM 500 MHz or 600 MHz spectrometers (Bruker, Ettlingen, Germany) in $CDCl_3$ using tetramethylsilane (TMS) as an internal reference standard. Chemical shifts (δ) have been expressed in ppm and the coupling constants (J) have been given in Hz. High-resolution electrospray mass spectroscopy was performed on a Thermo Scientific Q Exactive Orbitrap LC-MS/MS System (HR-ESI-MS) (Thermo Scientific, Waltham, MA, USA). High-performance liquid chromatography (HPLC) was conducted on an Ultimate 3000 HPLC system (Dionex Co., Sunnyvale, CA, USA) equipped with an Ultimate 3000 pump and Ultimate 3000 Variable Wavelength detector, as well as a semi-preparative YMC-Pack ODS-A column (250 × 10 mm, 5 μ m) and a preparative YMC-Pack ODS-A column (250 × 20 mm, 5 μ m) from YMC Co., Ltd (Kyoto, Japan). Column chromatography (CC) was conducted over silica gel (200–300 mesh and 300–400 mesh, Qingdao Haiyang Chemical Industry Co., Ltd., Qingdao, China). Chromatographic grade acetonitrile was purchased from Chang Tech Enterprise Co., Ltd (Taiwan, China). Dulbecco's Modified Eagle Medium (DMEM) and 0.25% pancreatin were obtained from Wuhan Procell Life Science Technology Co., Ltd. (Wuhan, China), the glucose kit was obtained from Shanghai Rongsheng Biotech Co., Ltd. (Shanghai, China), Metformin hydrochloride tablets were obtained from Sino-American Shanghai Squibb Pharmaceuticals Ltd. (Shanghai, China), Cell counting kit-8 (CCK8) was obtained from ABclonal Tech-

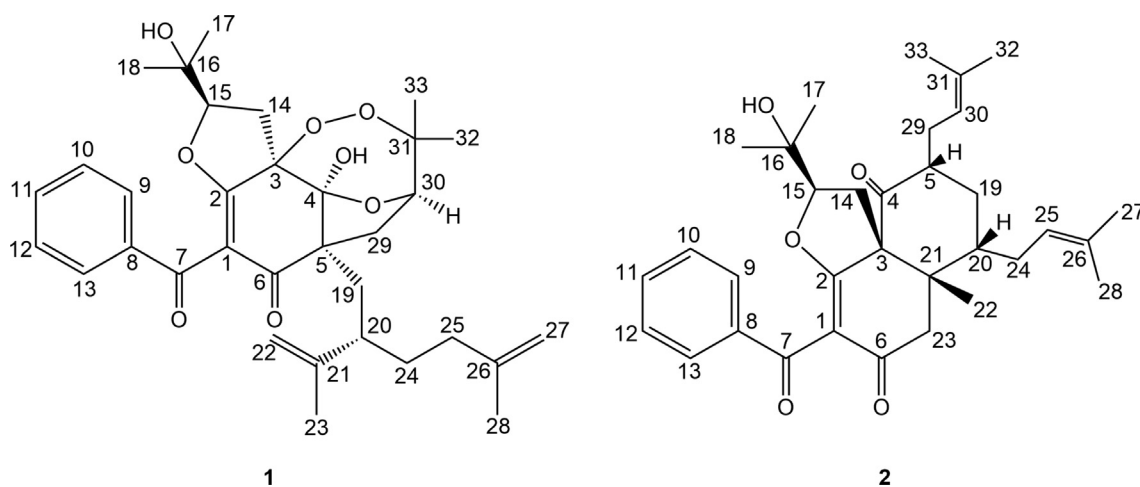


Fig. 1 Structures of compounds 1–2.

nology Co., Ltd. (Wuhan, China), Glucose solution and palmitic acid (PA) were obtained from Sigma-Aldrich Co., Ltd. (St. Louis, MO, USA), fetal bovine serum (FBS) was obtained from Zhejiang Tianhang Biotechnology Co., Ltd. (Hangzhou, China).

2.2. Plant material

Dried fruits of *G. bracteata* and *G. multiflora* were collected from Jinping County, Honghe Prefecture, Yunnan Province, and Nanning, Guangxi Zhuang Autonomous Region, P. R. China, respectively, which were identified by Prof. Hongli Teng, Guangxi Zhuang medicine international hospital and Prof. Hong Liu, College of Life Sciences, South Central University for Nationalities, respectively. The voucher specimen was deposited in the herbarium of School of Pharmaceutical Sciences, South Central University for Nationalities.

2.3. Extraction and isolation

Air-dried fruits of *G. bracteata* (10.4 kg) were extracted with 95% EtOH three times (12 h each time) at room temperature. The combined EtOH extracts were evaporated under vacuum to yield a brown-yellow crude gum (2.6 kg), and then suspended in H₂O and extracted with ethyl acetate (EtOAc) to yield an ethyl acetate-soluble portion (1.1 kg). The ethyl acetate-soluble portion was purified by silica gel column chromatography, using petroleum ether-EtOAc gradient (9:1, 8:2, 7:3, 1:1, 3:7, 0:1) as eluent, to yield 7 fractions (Fr. A-Fr. G). Fr. E (128 g) was loaded on silica gel CC eluted with P.E.-EtOAc (9:1, 8:2, 7:3, 1:1, 3:7, 0:1) to yield 6 fractions (Fr.E-1-Fr.E-6). Fr.E-4 was subjected to the repeated silica gel column and semipreparative HPLC to give compound **1** (5.3 mg, $t_R = 101.7$ min, 51% CH₃CN: H₂O).

The dried fruits of *G. multiflora* (5.2 kg) were powdered and extracted with 95% EtOH at room temperature three times (each time for 24 h) to obtain EtOH extract 2.21 kg, and then successively partitioned with petroleum ether (PE), EtOAc, and n-BuOH to get PE extracts 125 g, EtOAc extracts 166 g, n-BuOH extracts 80 g. The PE extracts (125 g) was chromatographed on a silica gel column (200–300 mesh) eluted successively with PE/acetone gradient (50:1, 25:1, 10:1, 7:3, 1:1, 0:1) to obtain 6 fractions (Fr. A-Fr. F). Fr. C was subjected to repeated silica gel CC with PE/CH₂Cl₂ (50:1 to 0:1), ODS CC with H₂O-MeOH (7:3 to 0:1) and semi-preparative HPLC to afford compound **2** (1.2 mg, $t_R = 10.2$ min, 87% MeOH: H₂O).

Garcibractinone C (**1**), white amorphous powder; $[\alpha]_D^{20} = +32.1^\circ$ (c 0.02, MeOH); UV (MeOH) λ_{\max} (log ϵ): 210 (3.83), 250 (3.99) nm; ECD (3.54 $\times 10^{-4}$ M, MeOH) $\lambda(\theta)$ 204 (+10.76), 238 (−0.72), 264 (+3.19), 316 (−4.44) nm; ¹H NMR (500 MHz, CDCl₃) and ¹³C NMR (125 MHz, CDCl₃) see Table 1; HR-ESI-MS m/z 587.2770 [M+Na] (calcd for C₃₃H₄₂O₈Na⁺, 587.2772).

Garmultinone E (**2**), white amorphous powder; $[\alpha]_D^{20} = +14.4^\circ$ (c 0.01, MeOH); UV (MeOH) λ_{\max} (log ϵ): 210 (4.05), 250 (4.24) nm; ECD (1.90 $\times 10^{-4}$ M, MeOH) $\lambda(\theta)$ 218 (+1.14), 243 (−8.14), 299 (+3.70) nm; ¹H NMR (600 MHz, CDCl₃) and ¹³C NMR (150 MHz, CDCl₃) see Table 1; HR-ESI-MS m/z 519.3106 [M+H]⁺ (calcd for C₃₃H₄₃O₅⁺, 519.3105).

2.4. NMR calculation

The calculated NMR was conducted using the Gauge-Including Atomic Orbitals (GIAO) method at the mPW1PW91/6-311+G (2d,p) level in chloroform with the IEFPCM model. This method was used as previously described (Tan et al., 2021).

2.5. ECD calculation

The absolute configurations of **1** and **2** were determined by quantum chemical TDDFT calculations of their theoretical ECD spectra. This method was used as previously described (Tan et al., 2021).

2.6. Cell viability

HepG2 cells (1.5 $\times 10^4$ cells/well) were grown in a 96-well plate in a DMEM medium containing 15% fetal bovine serum at 37 °C. After being treated with compound **1** at different levels (2, 4, 6, 8, and 10 μ M) for 24 h, the supernatant was discarded. Each well was added with 100 μ L DMEM and 10 % CCK8 at 37 °C for 30 min. The absorbance was measured at 450 nm with a microplate analyzer to calculate the cell survival rate.

2.7. Glucose consumption in IR-HepG2 cells

The IR-HepG2 cell model was induced by palmitic acid (PA) as previously reported (Nie et al., 2017). Briefly, after 12 h serum-free starvation, HepG2 cells were cultured in high glucose (30 mM) DMEM plus PA (0.25 mM) as the IR group, and high glucose DMEM plus PA in the presence of compound **1** with different concentrations (2, 4, and 6 μ M) for 24 h. The glucose concentration in the medium was measured using a glucose assay kit (Nanjing Jiancheng Bioengineering Institute) according to the instruction. The amount of glucose consumption was calculated by the initial glucose level minus the glucose level remaining in the medium (Yu et al., 2017). Metformin hydrochloride (10 μ M) was used as the positive control.

3. Results and discussion

Compound **1** was isolated as white amorphous powder. The molecular formula of **1** was determined as to be C₃₃H₄₂O₈ by analyzing its *pseudo* molecular ion peak at m/z 589.2770 ([M+Na]⁺, calcd for C₃₃H₄₂O₈Na⁺, 589.2772) of its HR-ESI-MS data, indicating 13 degrees of unsaturation (DOUs). The ¹H NMR combined with its HSQC spectrum of **1** (Figs. S2 and S5, SI, Table 1) displayed six tertiary methyls [δ_H 1.13 (s), 1.15 (s), 1.28 (s), 1.34 (s), 1.72 (s), 1.78 (s)], one monosubstituted phenyl group [δ_H 7.80 (2H, d, $J = 8.0$ Hz), 7.44 (2H, d, $J = 8.0$ Hz), 7.56 (1H, t, $J = 8.0$ Hz)], two olefinic methylenes [δ_H 4.73 (br s), 4.68 (br s); 5.04 (br s), 5.06 (br s)], two oxygenated methines [δ_H 4.58 (dd, $J = 10.0, 6.0$ Hz); 4.04 (dd, $J = 10.0, 4.5$ Hz)], and one hydroxyl group [δ_H 4.15 (s)]. Described analysis of ¹³C NMR, DEPT (Figs. S3–S4, SI) combined with its 2D-NMR spectra displayed 33 carbon signals that were assigned to a benzoyl group [δ_C 2 \times 129.3 (d), 2 \times 128.7 (d), 133.6 (d), 137.5(s), 191.4 (s)]; a ω -isogeranyl

Table 1 ^1H and ^{13}C NMR Spectroscopic Data for Compounds **1** and **2** in CDCl_3 .

No.	1^a		2^b	
	δ_{H}	δ_{C}	δ_{H}	δ_{C}
1		112.3		114.4
2		169.0		176.7
3		93.1		68.3
4		105.6		210.3
5		57.6	2.80 (1H, m)	45.5
6		198.4		194.0
7		191.4		193.5
8		137.5		137.9
9	7.80 (1H, d, $J = 8.0$ Hz)	129.3	7.99 (1H, d, $J = 8.0$ Hz)	129.6
10	7.44 (1H, t, $J = 8.0$ Hz)	128.7	7.47 (1H, t, $J = 8.0$ Hz)	128.7
11	7.56 (1H, t, $J = 8.0$ Hz)	133.6	7.56 (1H, t, $J = 8.0$ Hz)	133.5
12	7.44 (1H, t, $J = 8.0$ Hz)	128.7	7.47 (1H, t, $J = 8.0$ Hz)	128.7
13	7.80 (1H, d, $J = 8.0$ Hz)	129.3	7.99 (1H, d, $J = 8.0$ Hz)	129.6
14	2.93 (1H, dd, $J = 14.0, 6.0$ Hz); 2.85 (1H, dd, $J = 14.0, 10.0$ Hz)	26.3	2.58 (1H, dd, $J = 10.8, 12.6$ Hz); 2.16 (1H, dd, $J = 13.2, 5.4$ Hz)	29.5
15	4.58 (1H, dd, $J = 10.0, 6.0$ Hz)	92.5	4.16 (1H, dd, $J = 10.2, 5.4$ Hz)	90.3
16		71.8		70.2
17	1.15 (3H, s)	24.3	1.10 (3H, s)	24.6
18	1.13 (3H, s)	27.0	1.16 (3H, s)	27.2
19	2.03 (1H, m); 1.94 (1H, m)	39.3	2.25 (1H, m); 1.26 (1H, m)	33.8
20	2.32 (1H, m)	41.8	1.78 (1H, m)	44.1
21		151.5		44.7
22	5.06 (1H, br s); 5.04 (1H, br s)	114.5	1.34 (3H, s)	22.4
23	1.78 (3H, s)	19.8	2.37 (1H, d, $J = 16.2$ Hz); 2.24 (1H, m)	41.8
24	1.94 (2H, m)	35.8	2.23 (1H, m); 2.09 (1H, m)	27.9
25	1.56 (1H, m); 1.60 (1H, m)	35.5	5.12 (1H, m)	122.3
26		145.5		134.1
27	4.73 (1H, br s); 4.68 (1H, br s)	110.3	1.73 (3H, s)	26.0
28	1.72 (3H, s)	22.8	1.64 (3H, s)	18.2
29	2.82 (1H, dd, $J = 13.5, 3.5$ Hz); 2.31 (1H, m)	36.1	2.47 (1H, m); 2.09 (1H, m)	27.6
30	4.04 (1H, dd, $J = 10.0, 4.5$ Hz)	78.8	5.09 (1H, m)	120.9
31		87.9		134.5
32	1.34 (3H, s)	22.0	1.80 (3H, s)	26.0
33	1.28 (3H, s)	25.7	1.60 (3H, s)	18.1
4-OH	4.15 (s)			

group [δ_{C} 39.3 (t), 41.8 (d), 151.5 (s), 114.5 (t), 19.8 (q), 35.8 (t), 35.5 (t), 145.5 (s), 110.3 (t), 22.8 (q)]; an enolized 1,3-diketo moiety [δ_{C} 112.3 (s), 169.0 (s), 198.4 (s)]; one oxygenated tertiary carbon [δ_{C} 93.1 (s)]; one sp^3 quaternary carbon [δ_{C} 57.6 (s)]; one ketal carbon [δ_{C} 105.6 (s)], 3-hydroxy-2-oxygenated 3-methylbutyl group [δ_{C} 26.3 (t), 92.5 (d), 71.8 (s), 24.3 (q), 27.0 (q)] and 2, 3-dioxygenated 3-methylbutyl group [δ_{C} 36.1 (t), 78.8 (d), 87.9 (s), 22.0 (q), 25.7 (q)]. HMBC correlations (Fig.S6, SI, Fig. 2) from one hydroxyl group [δ_{H} 4.15 (s)] to δ_{C} 105.6 (s, C-4) and 93.1 (s, C-3), from H_2 -19 to δ_{C} 57.6 (s, C-5) and 105.6 (s, C-4), from H_2 -14 to δ_{C} 93.1 (s, C-3) and 169.0 (s, C-2), from H_2 -29 to δ_{C} 57.6 (s, C-5) and 198.4 (s, C-6) implied that an enolized 1,3-diketo group, one sp^3 quaternary [δ_{C} 57.6 (s)] and two oxygenated carbons [δ_{C} 105.6 (s), 93.1 (s)] constructed the phloroglucinol core. Moreover, these findings indicated that a ω -isogeranyl and 2, 3-dioxygenated 3-methylbutyl group were linked to C-5, and 3-hydroxy-2-oxygenated 3-methylbutyl group was linked to C-3 respectively. The remaining benzoyl group might be connected to C-1. In addition to the existence of three double bonds, two carbonyls, one phenyl and a six-membered ring, three DOUs

were needed to satisfy the molecular formula of **1**. These findings suggested that C-2, C-3 and C-4 of the phloroglucinol core were connected to C-15, C-30 and C-31 through ether bond or peroxy bond to establish the remaining three rings. Detailed the analysis of 2D-NMR data, 5 possible structures of the compound **1** could be easily obtained (Fig. 3). Compound **1** showed HMBC correlation from H-30 to δ_{C} 105.6 (s, C-4). After careful analysis of these five possible structures, it was found that there was a $^4J_{\text{HC}}$ “nonstandard” HMBC correlation between H-30 and C-4 in the structures 1–1, 1–4 and 1–5. It was easy to exclude these three structures. Moreover, GIAO NMR calculations for the five candidates were carried out to choose the most suitable structure. After NMR calculations of five candidate structures (Table S4, SI, Table 2), it is found that the candidate structure 1–2 showed the small values of the corrected mean absolute deviation (CMAD), the corrected largest absolute deviation (CLAD), and the root-mean-square deviation (RMSD) with 1.86, 5.8 and 2.36 respectively, and high correlation coefficients (R^2) of about 0.9981. These findings implied that the GIAO NMR calculations unequivocally defined structure 1–2 as the most likely structure

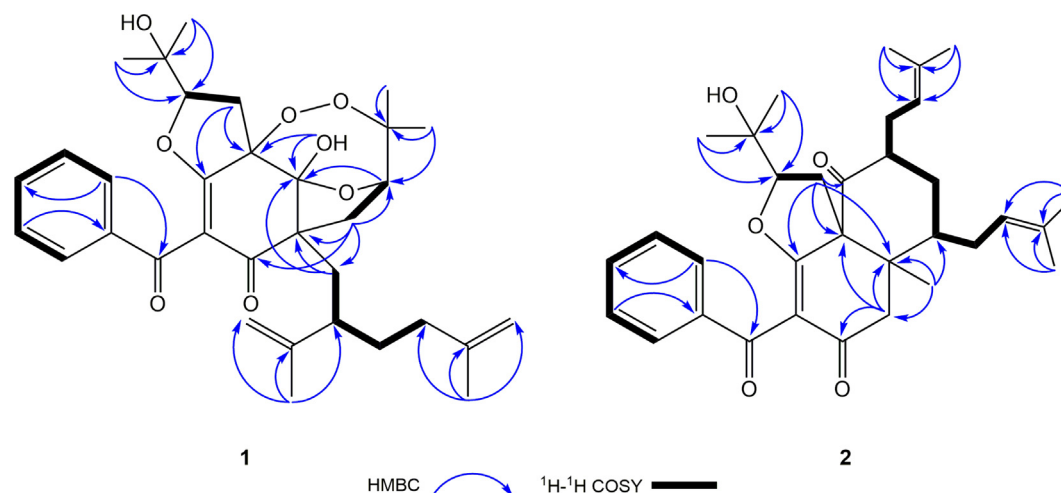


Fig. 2 Key HMBC and ^1H - ^1H COSY correlations of compounds **1** and **2**.

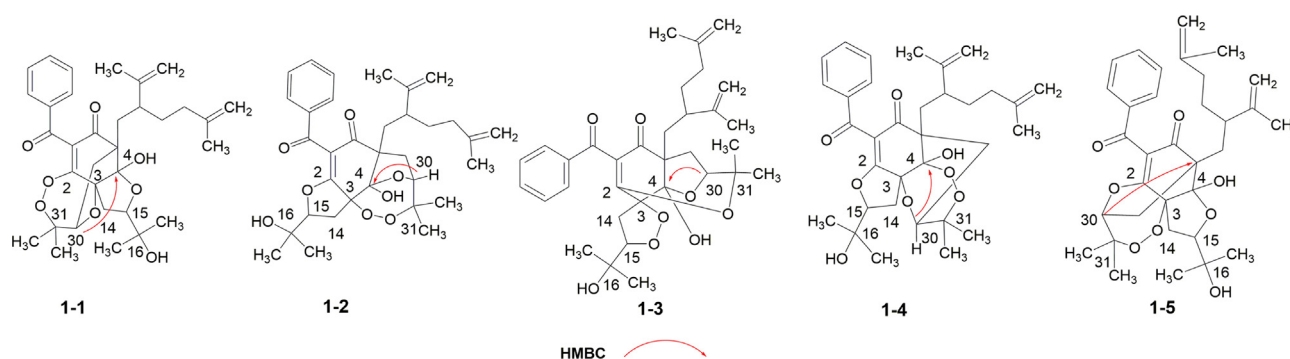


Fig. 3 Five candidates for **1** generated by 2D-NMR data.

Table 2 Statistics of Ordinary Least Squares Linear Regression (OLS-LR) of Experimental and Calculated ^{13}C NMR chemical shifts of compound **1**.

Compounds	CMAD	CLAD	R^2	RMSD
1-1	3.76	16.51	0.9906	5.31
1-2*	1.86	5.80	0.9981	2.36
1-3	3.99	19.82	0.9879	6.03
1-4	2.84	10.89	0.9946	4.02
1-5	5.42	19.38	0.9814	7.47
1a*	1.86	5.80	0.9981	2.36
1b	2.05	9.41	0.9971	2.96
1c	1.75	5.98	0.9983	2.23
1d	1.97	9.31	0.9973	2.87

* Compounds **1-2** and **1a** share the same structure.

among the five candidates. Thus, the 2D structure of **1** was assigned.

With the aid of the 2D structure of **1** established, the ROESY spectrum (Fig. S8, SI, Fig. 4) was employed to investigate the relative configuration of **1**. ROESY correlations of OH-4/ H_2 -19, OH-4/ H_2 -14, and H_2 -19/ H -30 suggested that ω -isogeranyl group at C-3, 4-OH, H-30, and H_2 -14 were cofacial. Moreover, ROESY correlations of OH-4/ CH_3 -23 and H-20 further confirmed this deduction. To further confirm the relative configurations of C-15 and C-20, four possible diastere-

omers for **1**: ($3R^*$, $4S^*$, $5S^*$, $15S^*$, $20S^*$, $30R^*$)-**1a**, ($3R^*$, $4S^*$, $5S^*$, $15S^*$, $20R^*$, $30R^*$)-**1b**, ($3R^*$, $4S^*$, $5S^*$, $15R^*$, $20S^*$, $30R^*$)-**1c**, ($3R^*$, $4S^*$, $5S^*$, $15R^*$, $20R^*$, $30R^*$)-**1d** were carried out by DP4+ analysis based on NMR calculations. As was obvious from these results shown in Table 2, the candidate structure **1c** showed the small values of the corrected mean absolute deviation (CMAD), the corrected largest absolute deviation (CLAD), and the root-mean-square deviation (RMSD) with 1.75, 5.98 and 2.23 respectively, and high correlation coefficients (R^2) of about 0.9983. Furthermore, ($3R^*$,

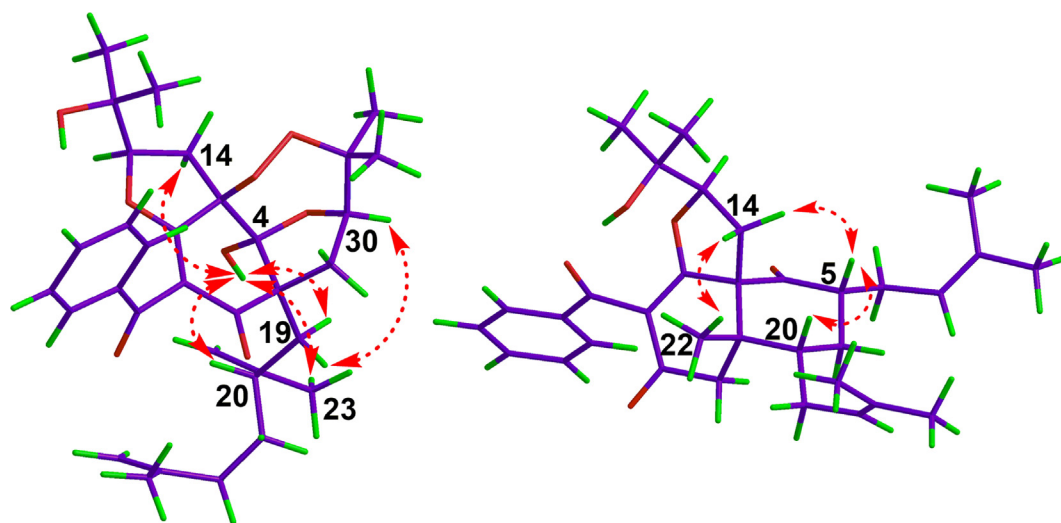


Fig. 4 ROESY correlations for compounds **1** (left) and **2** (right).

4*S**, 5*S**, 15*R**, 20*S**, 30*R**)-1c showed high DP4+ probability with 99.96%, suggesting the relative configurations of C-15 and C-20 as *R** and *S** respectively (Fig. S27, Table S5–S6, SI, Fig. 5). Therefore, the relative configuration of **1** was defined as (3*R**, 4*S**, 5*S**, 15*R**, 20*S**, 30*R**)). To further confirm the absolute configuration of **1**, the ECD calculations for (3*S*, 4*S*, 5*R*, 15*R*, 20*S*, 30*R*)-1c and its enantiomers were carried out through the TDDFT/ECD method at the B3LYP/6-31+G(d) level. As a result, the calculated ECD curves of (3*S*, 4*S*, 5*R*, 15*R*, 20*S*, 30*R*)-1c were in good agreement with the experimental ECD spectrum (Fig. 6). Thus, the absolute configuration of **1** was established as depicted in Fig. 1, and named garcibractinone C.

Compound **2** was isolated as a white amorphous powder. The molecular formula of **2** was determined to be C₃₃H₄₂O₅ by analyzing its *pseudo* molecular ion peak at *m/z* 519.3106 ([M+H]⁺, calcd for C₃₃H₄₃O₅⁺, 519.3105) of its HR-ESI-MS data, indicating 13 degrees of unsaturation (DOUs). Comparison of its NMR data (Figs. S12–17, SI) with those of **1** implied that they possessed a benzoyl group, an enolized 1,3-diketo moiety, and 2-(1-hydroxy-1-methylethyl)-tetrahydrofuran ring. Apart from the abovementioned signals, the remaining signals included a methyl group [δ_C 22.4 (q)], one nonconjugated carbonyl [δ_C 210.3 (s)], two *sp*³ quaternary carbons [δ_C 68.3 (s); 44.7 (s)]; two methylene groups [δ_C 33.8 (t); 41.8 (t)]; two methine groups [δ_C 44.1 (d); 45.5 (d)], and two prenyl groups [δ_C 27.6 (t), 120.9 (d), 134.5 (s), 26.0 (q), 18.1 (q); δ_C 27.9 (t), 122.3 (d), 134.1 (s), 26.0 (q), 18.2 (q)]. In addition to the existence of three double bonds, three carbonyls, one phenyl, and a five-membered ring, two DOUs were needed to satisfy the molecular formula of **2**. Therefore, compound **2** still had two more rings. HMBC correlations from CH₃-22 [δ_H 1.34 (s)] to δ_C 44.7 (s, C-21) and 41.8 (t, C-23), from H₂-14 to δ_C 68.3 (s, C-3), 44.7 (s, C-21) and 176.7 (s, C-2), from H₂-23 to δ_C 68.3 (s, C-3), 44.7 (s, C-21) and 194.0 (s, C-6) implied that an enolized 1,3-diketo moiety, two *sp*³ quaternary carbons [δ_C 68.3 (s); 44.7 (s)] and one methylene group [δ_C 41.8 (t)] established one six-membered ring with one methyl at C-21 and 2-(1-hydroxy-1-methylethyl)-tetrahydrofuran ring fused with C-2 and C-3 through ether linkage between C-15 and C-2 respec-

tively. From ¹H-¹H COSY, HSQC, and HMBC, the partial structure-CH(30)-CH₂(29)-CH(5)-CH₂(19)-CH(20)-CH₂(24)-

CH(25)- was deduced, suggesting that two prenyl groups were connected to C-5 and C-20 respectively. HMBC correlations from CH₃-22 to δ_C 45.5 (d, C-20) and H₂-14 to δ_C 210.3 (s, C-4) indicated that the carbonyl was connected to C-3, and the linkage between C-20 and C-21 was established. Two “loose ends” of C-4 (δ_C 210.3) and C-5 (δ_C 44.1) should be connected to construct the other six-membered ring. Thus, the 2D structure of **2** was defined. The relative configuration of **2** was established by analyzing the ROESY spectrum (Fig. S18, SI). ROESY correlations of CH₃-22 to CH₂-14, CH₂-14 to H-5, and H-5 to H-20 demonstrated CH₃-22 and CH₂-14 were on the same side defined as β -orientation, and 5, 20-diprenyl groups were on the other side defined as α -orientation. Owing to the lack of useful ROESY correlations, the relative configuration of C-15 could not be determined. Thus, to further verify the relative configuration of C-15, NMR calculations with the DP4+ analysis of two isomers (3*R**, 5*R**, 15*R**, 20*S**, 21*S**)-2a and (3*R**, 5*R**, 15*S**, 20*S**, 21*S**)-2b were carried out. The results indicated that (3*R**, 5*R**, 15*R**, 20*S**, 21*S**)-2a was the most likely structure for **2**, which had a small value of CLAD with 4.83, better correlation coefficient ($R^2 = 0.9985$), and had a high DP4+ probability of 100.00% based on all NMR data (Fig. S28, Table S7–S8, SI). Thus, the relative configuration of C-15 was fully identified as *R**. The ECD calculations for (3*R*, 5*R*, 15*R*, 20*S*, 21*S*)-2a and its enantiomer were performed using the TDDFT/ECD method at the B3LYP/6-31+G(d) level. The results showed that the calculated ECD data of (3*R*, 5*R*, 15*R*, 20*S*, 21*S*)-2a was in good agreement with the experimental ECD data (Fig. 7), suggesting **2** had the same corresponding absolute configuration. Thus, the absolute configuration of **2** was established as depicted in Fig. 1, and named garmultinone E.

The genus of *Garcinia* is a rich source of different types of PPAPs, and BPAPs are considered as the main constituents. As far as we know, compound **1** is the first example of 2, 3-dioxo [5.3.1]-type-BPAPs while **2** is the first example of [4.4.0]-type-BPAPs, which are completely inconsistent with

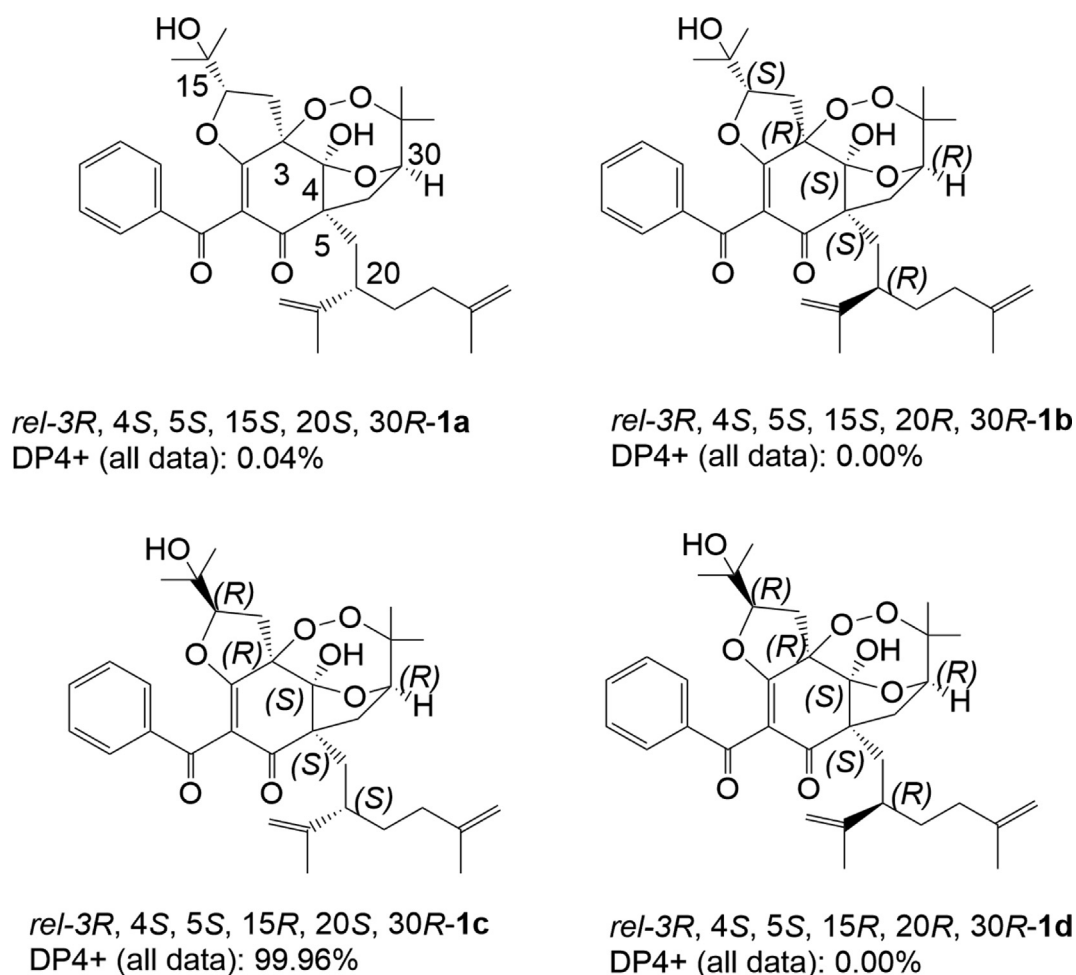


Fig. 5 DP4+ analysis of four possible diastereomers (**1a-1d**) for **1**.

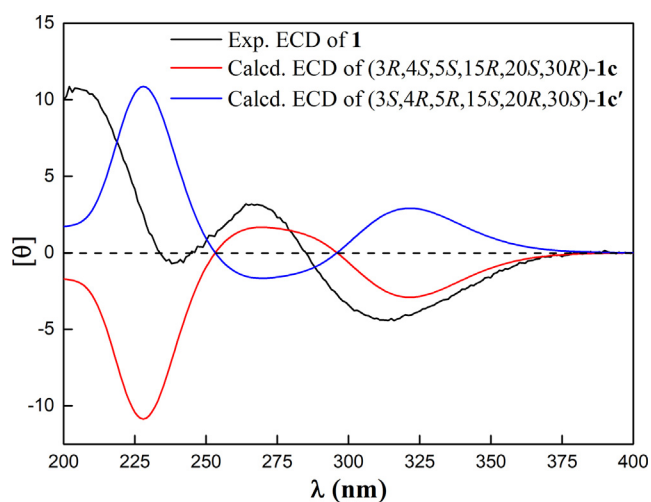


Fig. 6 Calculated and experimental ECD spectra of **1**.

the structural types of known PPAPs. According to biogenic analysis, both of them are derived from monocyclic polyprenylated acylphloroglucinol (MPAP). Starting from MPAP, it might undergo a series of oxidation, keto-enol tautomerism and cyclization reactions to produce the key intermediate *i*. Subsequently, an intramolecular nucleophilic addition reaction

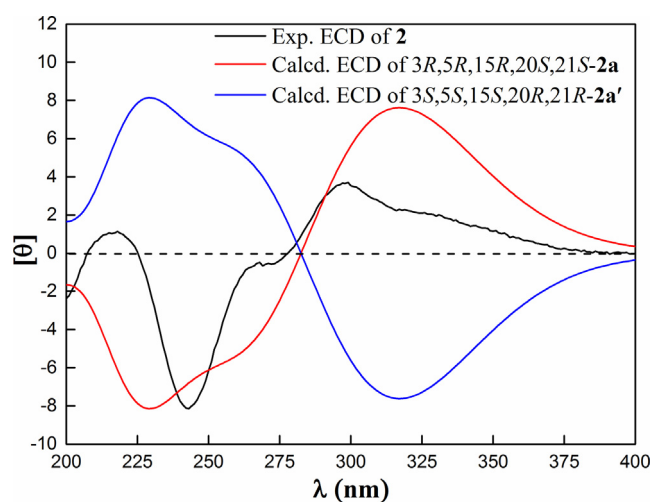


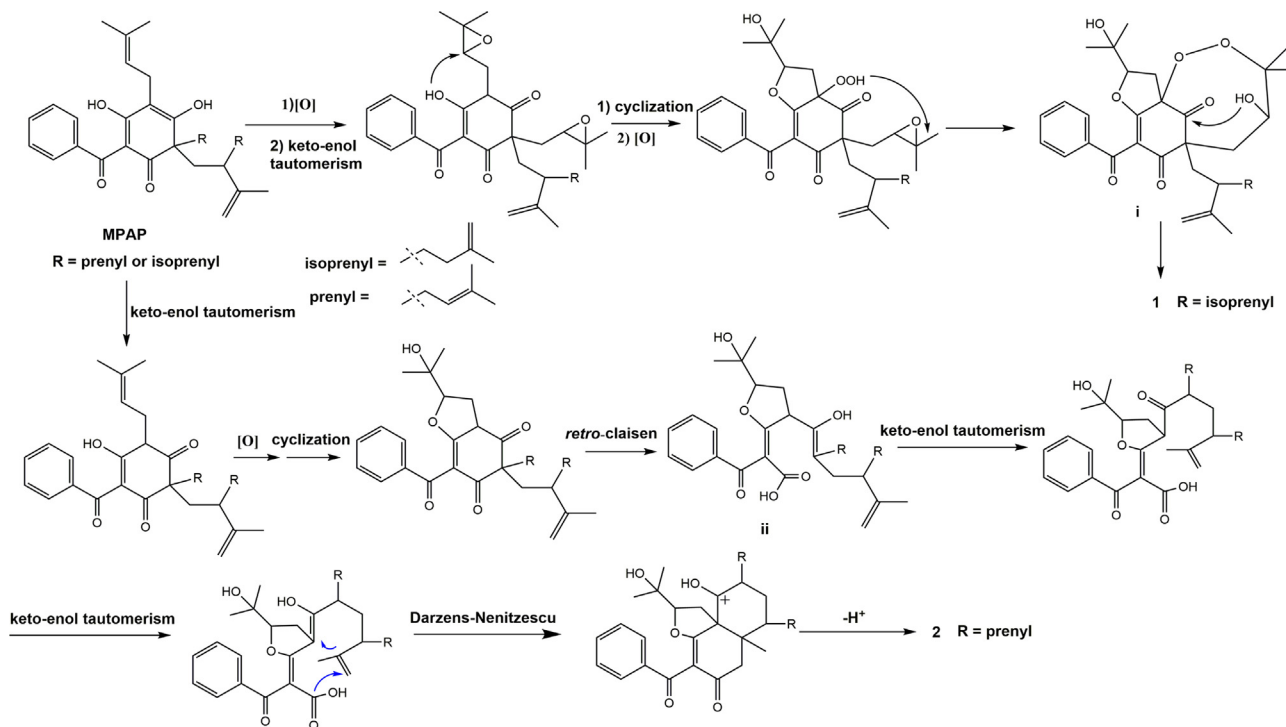
Fig. 7 Calculated and experimental ECD spectra of **2**.

occurred with the carbonyl group at C-4 and the hydroxyl group at C-30 to obtain **1**. In another way, MPAP could undergo a series of reactions, including keto-enol tautomerism, oxidation, cyclization, and *retro*-Claisen reaction, which resulted in C-5-C-6-carbon-carbon bond cleavage to give a key intermediate *ii*. Through a series of keto-enol tautomerism,

Darzens-Nenitzescu (Shono et al., 1983) and deprotonation reactions, it might be transformed into **2**. Thus, a plausible biosynthetic pathway for **1** and **2** was illustrated in Scheme 1.

Owing to the small amount of compound **2**, the biological activity of **2** was not tested. Compound **1** was evaluated for its hypoglycemic activity. IR is a typical feature of type 2 diabetes mellitus (T2DM) and refers to a decrease in glucose transport and metabolism in IR tissues such as the liver, skeletal muscle. HepG2 cells are human-derived hepatoblastoma cells that keep most functions of the liver and are widely used as IR models *in vitro* (Chen et al., 2021). Therefore, the hypoglycemic activity of **1** was assayed by the IR-HepG2 cell model. Firstly, cell viability was assessed by the CCK-8

method. As shown in Fig. 8A, the results indicated that **1** showed no cytotoxic effects on the viability of HepG2 cells at the concentration of 2, 4, and 6 μM (cell viability greater than 90%). Therefore, three concentrations of 2, 4, and 6 μM were used to treat IR-HepG2 cells. As shown in Fig. 8B, compared with the control group, the glucose consumption of the model group was significantly decreased, suggesting that the IR-HepG2 cell model was successfully built up. The glucose consumption of compound **1** at the concentration of 4 and 6 μM was 4.83 ± 0.43 and 5.45 ± 0.29 mM both of which were higher than that of the positive control of metformin (4.71 ± 0.42 mM). Moreover, the glucose consumption of **1** at the concentration of 6 μM was higher than the normal



Scheme 1 Plausible biosynthetic pathway for **1** and **2**.

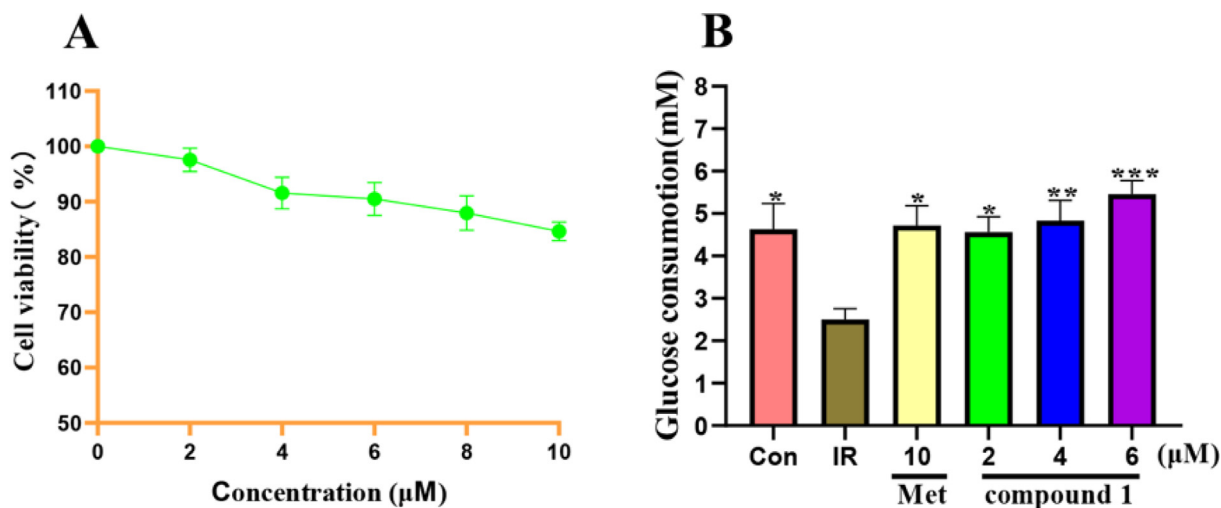


Fig. 8 (A) Effects of different concentrations of compound **1** on the viability of HepG2 cells. (B) Effects on glucose consumption in IR-HepG2 cells. * $p < 0.05$, ** $p < 0.01$ and *** $p < 0.001$ indicate significant differences from the IR group.

group. These findings showed that compound **1** could improve glucose metabolism disorders in IR-HepG2 cells.

4. Conclusions

In summary, PPAPs are considered to be important taxonomic markers in the *Guttiferae* family. Compounds **1–2**, possessing unique 6/5/7 and 6/6 ring systems with unprecedented 2, 3, 12-trioxatricyclo-[5.3.1.1^{5,11}] dodecane and bicyclo-[4.4.0] decane, were isolated from the fruits of *G. bracteata* and *G. multiflora* respectively. It is noteworthy that compound **1** is a highly oxidized PPAPs possessing a rare peroxide bond to form a seven-membered ring. Compound **2** belongs to 5, 6-*seco* PPAPs which is derived from a *retro*-claisen reaction. In the biosynthetic pathway of *nor*-PPAPs, *retro*-claisen and decarboxylation reaction were two key steps. However, it was very rare that the Darzens-Nenitzescu reaction replaced the decarboxylation reaction in the biosynthetic pathway of **2**. As a result, the carbon skeleton of **2** was completely different from the previously reported PPAPs. These findings enrich the chemical knowledge of the *Guttiferae* family. Through these putative biosynthetic pathways, more unprecedented PPAPs might be found from the *Guttiferae* family. Furthermore, the hypoglycemic activity of **1** was assayed by the IR-HepG2 cell model. The results showed that compound **1** at the concentrations of 2, 4, and 6 μM could significantly promote glucose uptake.

CRedit authorship contribution statement

Qingqing Li: Formal analysis, Writing – original draft. **Shuang Yang:** Formal analysis. **Haida Teng:** Formal analysis. **Xueni Li:** Formal analysis. **Wenli Xie:** Formal analysis. **Zhili Wu:** Formal analysis. **Guangzhong Yang:** Writing – review & editing. **Jing Xu:** Supervision, Writing – review & editing. **Yu Chen:** Supervision, Writing – review & editing.

Declaration of Competing Interest

The authors declare that they have no known competing financial interests or personal relationships that could have appeared to influence the work reported in this paper.

Acknowledgement

This work was supported by the National Key Research and Development Program of Hubei Province (2021ACB003), the Major Scientific and Technological Project of Hubei Province (2020ACA007) and the Special Fund for Basic Scientific Research of Central Colleges, South-Central University for Nationalities (CZY22002).

Appendix A. Supplementary material

Supplementary data to this article can be found online at <https://doi.org/10.1016/j.arabjc.2022.104137>.

References

Burns, D.C., Reynolds, W.F., 2021. Minimizing the risk of deducing wrong natural product structures from NMR data. *Magn. Reson. Chem.* 59, 500–533.

- Cao, V.A., Choi, B.K., Lee, H.S., 2021. Reisolation and structure revision of Asperspiropene A. *J. Nat. Prod.* 84, 1843–1847.
- Chen, J., Li, L., Zhang, X., Wan, L., Zheng, Q., Xu, D., Li, Y.T., Liang, Y., Chen, M.S., Li, B., Chen, Z.Y., 2021. Structural characterization of polysaccharide from *Centipeda minima* and its hypoglycemic activity through alleviating insulin resistance of hepatic HepG2 cells. *J. Funct. Foods* 82, 104478.
- Chhetri, B.K., Lavoie, S., Sweeney-Jones, A.M., Kubanek, J., 2018. Recent trends in the structural revision of natural products. *Nat. Prod. Rep.* 35, 514–531.
- Ciochina, R., Grossman, R.B., 2006. Polycyclic polyprenylated acylphloroglucinols. *Chem. Rev.* 37, 3963–3986.
- Grimblat, N., Zanardi, M.M., Sarotti, A.M., 2015. Beyond DP4: an improved probability for the stereochemical assignment of isomeric compounds using quantum chemical calculations of NMR shifts. *J. Org. Chem.* 80, 12526–12534.
- Marcarino, M.O., Cicetti, S., Zanardi, M.M., Sarotti, A.M., 2022. A critical review on the use of DP4+ in the structural elucidation of natural products: the good, the bad and the ugly. A practical guide. *Nat. Prod. Rep.* 39, 58–76.
- McAlpine, J.B., Chen, S.N., Kutateladze, A., MacMillan, J.B., Appendino, G., Barison, A., Beniddir, M.A., Biavatti, M.W., Bluml, S., Boufridi, A., Butler, M.S., Capon, R.J., Choi, Y.H., Coppage, D., Crews, P., Crimmins, M.T., Csete, M., Dewapriya, P., Egan, J.M., Garson, M.J., Genta-Jouve, G., Gerwick, W.H., Gross, H., Harper, M.K., Hermanto, P., Hook, J.M., Hunter, L., Jeannerat, D., Ji, N.Y., Johnson, T.A., Kingston, D.G.I., Koshino, H., Lee, H.W., Lewin, G., Li, J., Linington, R.G., Liu, M.M., McPhail, K.L., Molinski, T.F., Moore, B.S., Nam, J.W., Neupane, R.P., Niemitz, M., Nuzillard, J.M., Oberlies, N.H., Ocampos, F.M. M., Pan, G.H., Quinn, R.J., Reddy, D.S., Renault, J.H., Chavez, J. R., Robien, W., Saunders, C.M., Schmidt, T.J., Seger, C., Shen, B., Steinbeck, C., Stuppner, H., Sturm, S., Tagliatalata-Scafati, O., Tantillo, D.J., Verpoorte, R., Wang, B.G., Williams, C.M., Williams, P.G., Wist, J., Yue, J.M., Zhang, C., Xu, Z.R., Simmler, C., Lankin, D.C., Bisson, J., Pauli, G.F., 2019. The value of universally available raw NMR data for transparency, reproducibility, and integrity in natural product research. *Nat. Prod. Rep.* 36, 35–107.
- Nie, J.R., Chang, Y.N., Li, Y., Zhou, Y., Qin, J., Sun, Z., Li, H.B., 2017. Caffeic acid phenethyl ester (propolis extract) ameliorates insulin resistance by inhibiting JNK and NF- κ B inflammatory pathways in diabetic mice and HepG2 cell models. *J. Agric. Food Chem.* 65, 9041–9053.
- Phang, Y.L., Wang, X.Y., Lu, Y., Fu, W.W., 2020. Bicyclic polyprenylated acylphloroglucinols and their derivatives: structural modification, structure-activity relationship, biological activity and mechanism of action. *Eur. J. Med. Chem.* 205, 112646.
- Shono, T., Nishiguchi, I., Sasaki, M., Ikeda, H., Kurita, M., 1983. Novel acylation of aliphatic olefins promoted by active zinc compounds. *J. Org. Chem.* 48, 2503–2505.
- Socolsky, C., Plietker, B., 2015. Total synthesis and absolute configuration assignment of MRSA active garcinol and isogarcinol. *Chem. Eur. J.* 21, 3053–3061.
- Tan, X., Han, X.Y., Teng, H.D., Li, Q.Q., Chen, Y., Lei, X.X., Yang, G.Z., 2021. Structural elucidation of garcipaucinones A and B from *Garcinia paucinervis* using quantum chemical calculations. *J. Nat. Prod.* 84, 972–978.
- Yang, X.W., Grossman, R.B., Xu, G., 2018. Research progress of polycyclic polyprenylated acylphloroglucinols. *Chem. Rev.* 118, 3508–3558.
- Yu, Z., Chen, S., Wei, C., Chen, J., Ye, X., 2017. Proanthocyanidins from Chinese bayberry (*Myrica rubra* Sieb. et Zucc.) leaves regulate lipid metabolism and glucose consumption by activating AMPK pathway in HepG2 cells. *J. Funct. Foods* 29, 217–225.